Published in final edited form as:
J Immunol. 2008 July 15; 181(2): 1143–1152.

Enterocyte-Derived TAK1 Signaling Prevents Epithelium Apoptosis and the Development of Ileitis and Colitis

Rie Kajino-Sakamoto[*], **Maiko Inagaki**[*], **Elisabeth Lippert**[†], **Shizuo Akira**[‡], **Sylvie Robine**[§], **Kunihiro Matsumoto**[¶,‖], **Christian Jobin**[†], and **Jun Ninomiya-Tsuji**[*]

[*]Department of Environmental and Molecular Toxicology, North Carolina State University, Raleigh, NC 27695-7633 USA

[†]Department of Medicine and Center for Gastrointestinal Biology and Disease, University of North Carolina, Chapel Hill, NC 27510 USA

[‡]Department of Host Defense, Research Institute for Microbial Diseases, Osaka University, Osaka, JAPAN

[§]Morphogenesis and intracellular signalling, UMR 144, Institut Curie-CNRS, Paris, France

[¶]Department of Molecular Biology, Graduate School of Science, Nagoya University, Nagoya, 464-8602 JAPAN

[‖]Solution Oriented Research for Science and Technology (SORST), Japan Science and Technology Agency, Japan

Abstract

Recent studies have revealed that TAK1 kinase is an essential intermediate in several innate immune signaling pathways. In this study, we investigated the role of TAK1 signaling in maintaining intestinal homeostasis by generating enterocytes-specific constitutive and inducible gene deleted TAK1 mice. We found that enterocyte-specific constitutive TAK1 deleted mice spontaneously developed intestinal inflammation as observed by histological analysis and enhanced expression of IL-1β, MIP2 and IL-6 around the time of birth, which was accompanied by significant enterocytes apoptosis. When TAK1 was deleted in the intestinal epithelium of 4-week-old mice using an inducible knockout system, enterocytes underwent apoptosis and intestinal inflammation developed within 2–3 days following the initiation of gene deletion. We found that enterocytes apoptosis and intestinal inflammation were strongly attenuated when enterocyte-specific constitutive TAK1 deleted mice were crossed to TNF receptor 1 (TNFR1)−/− mice. However, these mice later (>14 days) developed ileitis and colitis. Thus, TAK1 signaling in enterocytes is essential for preventing TNF-dependent epithelium apoptosis and the TNF-independent development of ileitis and colitis. We propose that aberration in TAK1 signaling might disrupt intestinal homeostasis and favor the development of inflammatory disease.

Keywords

Rodent; Apoptosis; Cytokines; Inflammation; Mucosa

To whom correspondence should be addressed:, Jun Ninomiya-Tsuji, Department of Environmental and Molecular Toxicology, North Carolina State University, Campus Box 7633, Tel: 919-513-1586, Fax: 919-515-7169, Jun_Tsuji@ncsu.edu.

Introduction

Intestinal epithelium acts as a barrier against commensal and pathogenic bacteria by physically preventing their invasion as well as by activating the innate immune system to control bacterial colonization (1–4). Commensal bacteria constantly stimulate enterocytes through Toll-like receptors and intracellular bacterial sensors such as NODs. This stimulation is believed to be important in maintaining the physical barrier and to promote expression of cytokines/chemokines under steady-state conditions. Dysregulation of the innate immunity and loss of the intestinal physical barrier cause bacterial invasion and excessive production of cytokines/chemokines, which are associated with chronic inflammatory diseases such as inflammatory bowel disease (IBD) (5,6).

Transforming growth factor β-activated kinase 1 (TAK1) is an essential intermediate of innate immune signaling pathways. TAK1 is activated by Toll-like receptor ligands, as well as by inflammatory cytokines such as TNF and IL-1 (7–9). Furthermore, we have recently identified that TAK1 is also activated by the intracellular bacterial sensor NOD2 in skin epithelial cells (10). Following activation, TAK1 stimulates signaling pathways leading to the activation of two groups of transcription factors, AP-1 and NF-κB, which results in increased production of cytokines/chemokines. Therefore, it might be expected that TAK1 would play an important role in maintaining epithelial barrier function by this regulation of cytokines/chemokine production. In addition, it has been demonstrated that TAK1 deficiency results in an increased sensitivity to TNF-mediated apoptosis in fibroblasts and keratinocytes (8,9,11), which could be involved in tissue damage as discussed below.

Among inflammatory cytokines, TNF has a unique ability to induce cell death and tissue damage (12,13). TNF activates two opposing intracellular signaling pathway; one which activates anti-apoptotic pathways through the transcription factors NF-κB and AP-1; and another which induces caspase-dependent apoptosis through Fas-associated death domain (FADD) and pro-caspase 8 (also called FLICE) (12,14). TNF can presumably cause tissue damage when this pro-apoptotic pathway is predominantly activated. Indeed, TNF is closely associated with tissue damage in chronic inflammatory diseases, and anti-TNF therapy has been proven to be effective to reduce tissue damage (15). However, in most types of cells, TNF does not induce apoptosis because the anti-apoptotic pathway overrides the pro-apoptotic pathway (14). In the normal intestinal epithelium, TNF, even at very high concentration, cannot cause any damage (16). Thus, the mechanism by which TNF promotes tissue damage in chronic inflammatory diseases has not fully been elucidated.

We speculate that TAK1 may regulate intestinal epithelial integrity by controlling innate immunity in enterocytes and by modulating TNF-induced apoptosis and tissue damage. In this study, we examined the role of TAK1 in the intestinal epithelium by generating and characterizing mice with an intestinal enterocyte-specific deletion of TAK1. We found that deletion of TAK1 causes TNF-dependent tissue damage. We also found that enterocyte-derived TAK1 signaling is essential for preventing the TNF-independent development of ileitis and colitis.

Materials and Methods

Mice

Mice carrying a floxed *Map3k7* allele (*TAK1*$^{FL/FL}$) (17) with a C57BL/6/129 mixed background were used for generating *villin-CreTAK1*$^{FL/FL}$ and *villin-CreTAK1*$^{FL/FL}$ *TNFR1*$^{-/-}$ mice. We also generated *villin-CreTAK1*$^{FL/FL}$ and *villin-CreTAK1*$^{FL/FL}$ *TNFR1*$^{-/-}$ mice using *TAK1*$^{FL/FL}$ that were backcrossed to C57BL/6 for at least 5 generations, and we confirmed that the same phenotypes were observed using the

backcrossed *TAK1*$^{FL/FL}$ mice. The backcrossed *TAK1*$^{FL/FL}$ mice were use to generate *villin-CreER*^{T2}*TAK1*$^{FL/FL}$ mice. Mice carrying a *villin-Cre* with a C57BL/6 background (18) were from Jackson Lab, *villin-CreER*^{T2} with a C57BL/6 background were described previously (19), and TNFR1-deficient mice *C57BL/6 Tnfrsf1atm1Mak* (*TNFR1*$^{-/-}$) (20) were from Jackson Laboratory. In all experiments, littermates were used as controls. To induce recombination, 4-week-old mice were given intraperitoneal injections of tamoxifen (1 mg per 20 g body weight) for 2 to 3 consecutive days. Mice were bred and maintained under specific pathogen-free conditions. All animal experiments were done with the approval of the North Carolina State University Institutional Animal Care and Use Committee.

Histology

Sections from the small intestine (jejunum and ileum) and the colon (proximal and distal) were stained with hematoxylin and eosin for histological analysis. Mucosal inflammation was evaluated in cross-sections of the small intestine and the colon separately. Sections were scored in a blinded fashion on a scale from 0 to 4, based on the degree of lamina propria mononuclear cell infiltration, crypt hyperplasia, goblet cell depletion and architectural distortion, as previously described (21). To detect apoptotic cells, TUNEL assay was performed on paraffin sections using the DeadEnd™ Colorimetric TUNEL System (Promega) according to the manufacturer's instructions. Immunofluorescence was performed on frozen sections using polyclonal antibody against cleaved caspase 3 (1:200, Cell Signaling), TAK1 (1:200) (Ninomiya-Tsuji 1999), lysozyme (1:200, Novocastra), Ki67 (1:500, Novocastra), synaptophysin (1:100, Thermo Scientific), and monoclonal antibody against Nidogen (1:1000, Chemicon). Bound antibodies were visualized by Cy2- or Cy3-conjugated secondary antibodies against rabbit (1:500, GE healthcare) or rat (1:100, Chemicon). Nuclei were counterstained with DAPI. For the detection of intestinal goblet cells, paraffin-embedded sections were stained with Alcian Blue and with Nuclear Fast Red as counterstain.

Isolation of enterocytes

Enterocytes were isolated as described previously (22,23). Briefly, the whole small intestine was harvested and flushed with PBS to remove fecal contents. One end of the intestine was tied off, filled with Hanks' Balanced Salt Solution (HBSS, Sigma-Aldrich) containing 10 mM EDTA and incubated in a PBS bath at 37°C for 5 min. After removing the contents, the intestine was filled with PBS containing 1.5 mM EDTA and 0.5 mM DTT and incubated in PBS again for 10 min. The contents were collected into tubes and centrifuged at 1,200 rpm for 5 min. The resulting pellets containing predominantly epithelial cells were washed twice in cold PBS.

Immunoblot analysis

Enterocytes isolated from the small intestine were lysed in an extraction buffer (20 mM HEPES, pH 7.4, 150 mM NaCl, 12.5 mM β-glycerophosphate, 1.5 mM $MgCl_2$, 2 mM EGTA, 10 mM NaF, 2 mM dithiothreitol, 1 mM Na_3VO_4, 1 mM phenylmethylsulfonyl fluoride, 100 units/ml aprotinin, 0.5% Triton X-100). Proteins from cell lysates were electrophoresed by SDS-PAGE and transferred to Hybond-P (GE Healthcare). The membranes were immunoblotted with a polyclonal antibody against TAK1 described previously (7) and a monoclonal antibody against β-actin (Sigma). Bound antibodies were visualized with horseradish peroxidase-conjugated antibodies against rabbit or mouse IgG using the ECL Western blotting system (GE).

Genomic DNA analysis

Isolated enterocytes and liver, kidney and heart were roughly disrupted in lysis buffer (50 mM Tris-HCl, pH 7.4, 100 mM EDTA, pH 8.0, 100 mM NaCl, 1% SDS). The following primers were used: floxed TAK1, GGCTTTCATTGTGGAGGTAAGCTGAGA and GGAACCCGTGGATAAGTGCACTTGAAT; villin-Cre, GTGTGGGACAGAGAACAAACC and ACATCTTCAGGTTCTGCGGG; villin-CreER^{T2}, CAAGCCTGGCTCGACGGCC and CGCGAACAT CTTCAGGTTCT; truncated TAK1 (TAK1Δ), CACCAGTGCTGGATTCTTTTTGAGGC and GGAACCCGTGGATAAGTGCACTTGAAT.

Quantitative Real-time PCR

Total RNA from the ileum and middle of the colon were isolated using RNeasy Mini (Qiagen). cDNA was synthesized using TaqMan reverse transcription reagents (Applied Biosystems). mRNA levels of a non-truncated (full length) form of TAK1 were analyzed by real-time PCR with SYBR Green (Applied Biosystems). Full-length TAK1 primers, CGTCTTCTGCCAGTGAGATG (in the exon1) and ATCTTTTGCTCTCCACTTAGCTT (in the exon 2 flanked by *loxP*); glyceraldehyde-3-phosphate dehydrogenase (GAPDH) primer, GAAGGTCGCTGTGAACGGA and GTTAGTGGGGTCTCGCTCCT were used. Expression levels of IL-1β, IL-6, MIP2, S100A9 and TNF were also analyzed by TaqMan gene expression assay (Applied Biosystems). Results were analyzed using the comparative Ct Method. All values were normalized to the level of GAPDH messenger RNA.

ELISA

Frozen jejunum were ground into powder in liquid nitrogen, homogenized in cold-PBS containing a protease inhibitor cocktail (Calbiochem) and centrifuged at 14,000rpm, 4 °C for 5 min. Protein concentrations were determined by BCA Protein Assay Reagent Kit (PIERCE). IL-6 and IL-1β levels were analyzed using commercially available mouse IL-6 and IL-1b kits, respectively (BD Bioscience). ELISA was performed following manufacture's instruction. IL-6 and IL-1β levels were standardized to the total protein amount and data presented as ng of cytokine per mg of total protein.

Statistical analysis

Statistical comparisons were made using paired or independent, two-tailed Student's t-tests assuming equal variance and two-tailed Welch's t-tests assuming unequal variance.

Results

Intestinal epithelium-specific deletion of TAK1 causes intestinal damage

TAK1 is ubiquitously expressed in the intestinal tissues including intestinal epithelium, lamina propria, and smooth muscle, at least from embryonic day 16.5 (E16.5) to the adult stage (Fig. 1a and data not shown). To investigate TAK1 function in the intestinal epithelium, we generated mice lacking functional TAK1 specifically in enterocytes. Mice carrying loxP-flanked TAK1 allele (*TAK1^{FL}*) (17) were crossed with *villin*-Cre transgenic mice (18) to generate *villin-CreTAK1$^{FL/FL}$* mice. In this floxed TAK1 system, Cre recombinase catalyzes the deletion of the TAK1 ATP binding site, amino acids 41–77, resulting in the generation of a truncated/kinase-dead form of TAK1 (TAK1Δ) (11,17). In *villin-CreTAK1$^{FL/FL}$* mice, we anticipate that a truncated/kinase-dead version of TAK1 (TAK1Δ) is expressed in enterocytes, while a wild-type TAK1 is expressed in other cell types. We note that earlier studies have revealed that TAK1 deletion mice in that entire TAK1 expression is abolished (24–26) exhibit the same phenotypes as this TAK1 deletion (TAK1Δ/Δ) mice in embryos and T cells, (8,17). Since neonatal *villin-CreTAK1$^{FL/FL}$* mice

died as described below, we were not able to isolate enterocytes. To determine whether TAK1 is deleted in enterocytes, we performed several experiments using *villin-CreER^{T2}TAK1$^{FL/FL}$* (inducible KO) and *villin-CreTAK1$^{FL/FL}$ TNFR1$^{-/-}$* (DKO) mice, which will be described later.

villin-CreTAK1$^{FL/FL}$ mice were born at the expected Mendelian ratio, however they showed severe intestinal bleeding within 1 day of birth and died by P1. The small intestine and the colon from *villin-CreTAK1$^{FL/FL}$* mice showed hemorrhage at P0, while the intestine was grossly normal at E18.5 (Fig. 1b). The lengths of the small intestine and the colon were shorter in *villin-CreTAK1$^{FL/FL}$* mice at P0 than in control *TAK1$^{FL/FL}$* mice (Fig. 1c), while the colon length at E18.5 was not significantly different (data not shown). The control *TAK1$^{FL/FL}$* mice, as well as mice with intestinal epithelium-specific heterozygous deletion of TAK1 (*villin-CreTAK1$^{FL/+}$*), did not show any gross abnormalities (data not shown). The small intestine and colon of *villin-CreTAK1$^{FL/FL}$* mice at E15.5 and E17.5 were indistinguishable from control mice (data not shown). Histological analysis revealed that the small intestine and the colon showed evidence of inflammation at both E18.5 and P0 with architecturally disrupted epithelium and enhanced immune cell infiltration (Fig. 1d and e). We found that villi and crypts are formed normally in *villin-CreTAK1$^{FL/FL}$* mice by E18.5 (Fig. 1e) with no difference in crypts-villi length between control and mutant mice at E18.5 (Fig. 1f).

Therefore, we assume that intestinal development is not altered by deletion of TAK1. To further examine intestinal epithelium differentiation, we stained goblet cells and enteroendocrine cells. We also examined the level of metalloproteinase 7 (paneth cell marker) and neurogenin 3 (enteroendocrine cell marker). The numbers of goblet cells (Fig. 1g) and enteroendocrine cells (Fig. 1h) and the expression levels of metalloproteinase 7 and neurogenin 3 (Fig. 1i) were not markedly altered by TAK1 deletion. These data suggest that TAK1 is largely dispensable for cell fate decision during differentiation. Therefore, TAK1-deletion-induced intestinal epithelial damage is not due to a defect in development or differentiation. We note that the size of the goblet cells was found to be smaller in *villin-CreTAK1$^{FL/FL}$* mice than those in the control animals (Fig. 1g). Because it is known that goblet cell maturation is disrupted by inflammation, this may be a consequence of inflammatory conditions rather than a direct effect of TAK1 deletion.

Mice with intestinal epithelium-specific deletion of TAK1 show increased apoptotic cell number and inflammation

We speculated that the intestinal structural damage observed in *villin-CreTAK1$^{FL/FL}$* mice might be associated with cell death leading to inflammation. To verify these possibilities, we examined apoptosis by TUNEL assay as well as staining of cleaved caspase 3, and quantitated expression of inflammatory genes. The numbers of apoptotic cells markedly increased in all sections of the small intestine and the colon from *villin-CreTAK1$^{FL/FL}$* mice at P0 compared to *TAK1$^{FL/FL}$* mice (Fig. 2a and b). The pro-inflammatory chemokine MIP2 and chemotactic factor S100A9 were markedly up-regulated in the *villin-CreTAK1$^{FL/FL}$* small intestine and colon at P0 (Fig. 2c). At E18.5, we observed significant variability among individual mice, with some *villin-CreTAK1$^{FL/FL}$* mice exhibiting a striking increase in apoptotic cell number (Fig. 2a and b). Increased apoptosis correlated with the upregulation of proinflammatory cytokines and chemokines/chemotactic factors (Table 1). No apoptotic cells were detected at E16.5 and E17.5 (data not shown). These results demonstrate that apoptosis and inflammation are concomitantly induced around E18 in mice harboring an intestinal epithelium-specific deletion of TAK1.

TAK1 is required for prevention of apoptosis and inflammation in 4-week-old mice

Because of the severe intestinal damage observed at P0 in *villin-CreTAK1*$^{FL/FL}$ mice, we next utilized an inducible Cre-mediated recombination system to fully assess the role of TAK1 in adult mice. Mutant mice were generated by crossing *TAK1*$^{FL/FL}$ mice with *villin-CreER*^{T2} transgenic mice expressing a tamoxifen-dependent recombinase (*CreER*^{T2}) under the control of the intestinal epithelium-specific villin promoter (19). In this system, a mutant version of TAK1 (TAK1Δ) is generated in villin-expressing cells when mice are treated with tamoxifen. In the absence of tamoxifen, *villin-CreER*^{T2}*TAK1*$^{FL/FL}$ mice did not develop any spontaneous phenotype at least by the age of 8 months. We treated *villin-CreER*^{T2}*TAK1*$^{FL/FL}$ mice with tamoxifen at the age of 4 weeks and observed that TAK1 was effectively deleted (Fig. 3a–c).

Interestingly, *villin-CreER*^{T2}*TAK1*$^{FL/FL}$ mice developed pathological conditions associated with movement disorder, weight loss, and a mild diarrhea at only 3 days of consecutive injection of tamoxifen. At day 2, *villin-CreER*^{T2}*TAK1*$^{FL/FL}$ mice were grossly normal and did not lose weight. However, histological analysis of *villin-CreER*^{T2}*TAK1*$^{FL/FL}$ mice showed that the structure of the small intestine was disrupted at day 2 (Fig. 3d), and completely absent by day 3 (Fig. 3d). The colon structure of *villin-CreER*^{T2}*TAK1*$^{FL/FL}$ mice was relatively normal compared to the small intestine at day 2–3 (Fig. 3d). To examine whether apoptosis and inflammation were associated with this intestinal damage, we measured apoptosis by TUNEL assay and caspase 3 processing, and measured proinflammatory cytokines/chemokines/chemotactic mRNA levels. At day 2, apoptotic cells were markedly increased in the small intestine of the inducible TAK1 mutant mice, especially in the crypts (Fig. 3e and f). Apoptotic cells were more scattered in the small intestine at day 3, because most of epithelial cells had already been removed (Fig. 3e and f). In the colon, the number of apoptotic cells was higher at day 3 compared to at day 2, and apoptotic cells were observed mostly in the crypts. The levels of proinflammatory cytokines/chemokines/chemotactic factors were up-regulated in the small intestine at day 2–3 (Fig. 3g and data not shown). The inflammatory gene expression was increased in the colon of inducible TAK1 mutant mice at day 2–3 (Fig. 3g). In addition, CD4+ T lymphocytes, macrophages and dendritic cells were detected in the small intestine of TAK1 deleted mice at day 3 (data not shown). These results demonstrate that TAK1 is essential for preventing enterocyte death and development of intestinal inflammation not only in neonatal but also in 4-week-old mice.

The severity of intestinal damage and inflammation in the 4-week-old inducible TAK1 mutant mice after only 3 days of tamoxifen administration (Fig. 3d) was greater than that observed in the E18.5 non-inducible TAK1 mutant mice (Fig. 1e). Because genetic recombination was initiated at E12.5 in the embryonic midgut and highgut of non-inducible *villin-Cre* mice (18), we had expected that deletion of the TAK1 allele would have been efficiently induced before E18.5 in *villin-CreTAK1*$^{FL/FL}$ mice. However, we could not detect pronounced increase in apoptosis by E18.5-P0 in the TAK1 mutant mice. We speculated that 4-week-old mice might express higher levels of some apoptotic inducer(s) than the neonatal mice. We examined the level of one of best-known apoptotic inducers, TNF, in the embryonic, neonatal and 4-week-old intestine by real-time PCR. We note that TNF expression was not altered by genotype. Unlike other proinflammatory cytokines such as IL-1 and IL-6, TNF was not greatly up-regulated by TAK1 deletion (data not shown). However, we found that TNF expression was greatly increased in all genotype mice as mice grew (Fig. 4). The levels of TNF seem to be correlated with the severity of intestinal damage in the TAK1 mutant mice. Therefore, we assume that TNF may cause intestinal cell death and inflammation in mice lacking TAK1 expression in the intestinal epithelium.

Apoptosis and inflammatory defects caused by TAK1 deletion are rescued by inhibition of TNF signaling

To verify the hypothesis that the phenotype observed in TAK1-deficient mice is due to TNF-induced cell death, we generated double-mutant mice harboring a deletion of the *TNFR1* and containing *villin-CreTAK1*$^{FL/FL}$ (*villin-CreTAK1*$^{FL/FL}$ *TNFR1*$^{-/-}$). Deletion of the TAK1 gene in the double-mutant mice was confirmed by immunoblot in isolated enterocytes and mRNA analysis in the whole intestine (Fig. 5a and b). We found that the intestinal damage observed in *villin-CreTAK1*$^{FL/FL}$ neonatal mice was completely rescued by deletion of TNFR1 (Fig. 5c). Few or no apoptotic cells were detected in the double-mutant intestine (Fig. 5d) and the levels of cytokines/chemokines/chemotactic factors were similar in the double-mutant intestine compared to those in the control *TAK1*$^{FL/FL}$ *TNFR1*$^{-/-}$ mice (Fig. 5e). Goblet cells were also normal in the double mutant mice (Fig. 5f). These results indicate that TNF is a major cause of apoptosis and inflammation induced in the intestine harboring an epithelium-specific deletion of TAK1.

Double-mutant mice harboring intestinal epithelium-specific TAK1 deletion and TNFR1 deletion spontaneously develop ileitis and colitis

While abnormalities detected in *villin-CreTAK1*$^{FL/FL}$ neonatal mice were completely rescued by deletion of TNFR1 deletion, we noticed that weight gain was reduced in *villin-CreTAK1*$^{FL/FL}$ *TNFR1*$^{-/-}$ mice compared to control *TAK1*$^{FL/FL}$ *TNFR1*$^{-/-}$ mice at around the age of 2–3 weeks (Fig. 6a). Histological analysis in the double-mutant mice that had lost weight revealed that they developed ileitis and severe colitis (Fig. 6c). These double-mutant mice showed shorter colon length (Fig. 6b), an enlargement of crypt cellularity in the small intestine (Fig. 6d), and decrease of mature goblet cells (Fig. 6h). We found that apoptotic cells were more numerous in the double-mutant mice (Fig. 6e and f) and proinflammatory cytokines/chemokines/chemotactic factors were up-regulated (Fig. 6g). Despite the enlargement of crypt cellularity, the number and distribution of paneth cells were found to be normal in the double-mutant mice (Fig. 6i). This suggests that TAK1 deletion does not alter the differentiation of intestinal cells but causes hyperplasia in the intestine. We detected increased cellular proliferation in all regions of the small intestine and colon of the double-mutant mice (Fig. 6j). This hyperplasia could be due to compensatory cell proliferation induced by apoptosis and results of the proinflammatory milieu in these double mutant mice. These results suggest that, even in the absence of TNF signaling, TAK is important for preventing dysregulation in the intestinal epithelium, and its ablation causes ileitis and colitis.

Discussion

It has been established that NF-κB is an important mediator of cell survival (14,27). Abrogation of the NF-κB pathway by knockout of IKKβ or NEMO (IKKγ) causes hypersensitivity to TNF-killing (28–30). In skin epidermis, deletion of NEMO causes TNF-dependent cell death and thereby induces an inflammatory skin condition (31). This pathology is very similar to that seen in mice having a skin epidermal-specific deletion of TAK1 (11). TAK1 is an essential kinase in several intracellular signaling pathways and functions upstream of IKK-NF-κB (7–9). This similarity in phenotypes between TAK1-mutant and NEMO-mutant mice clearly indicates that TAK1-IKK-NF-κB is a major pathway that prevents TNF-induced killing in the skin epidermis. In contrast, mice with NEMO deletion in the intestinal epithelium have a phenotype that is somewhat different from mice having an intestinal epithelium-specific deletion of TAK1, even though NEMO and TAK1 were deleted by using the same *Villin-Cre* transgenic mice. Intestinal epithelium with a NEMO deletion slowly developed abnormalities including colitis in the colon by the age of 6 weeks (23). Cell death is detected in only a few scattered areas (23). In contrast, as

shown in this report, deletion of TAK1 in the intestinal epithelium almost immediately results in the death of enterocytes in the presence of TNF. This suggests that, although NF-κB is partly involved in the survival of enterocytes, TAK1 is more critical to determining their death or survival. Because TAK1 can activate not only NF-κB but also AP-1, AP-1 could be critically involved in enterocyte survival.

TAK1 deletion in the intestinal epithelium causes apoptosis and inflammation before birth, suggesting that the intestinal microbiota is not involved in this inflammatory condition. Because enterocyte apoptosis and intestinal inflammation was prevented in TNFR1 deleted mice, we concluded that TNF expressed in the intestine is the major cause of epithelial damage in TAK1 deleted mice. However, we found that, even in the absence of TNF signaling, TAK1 deletion causes ileitis and colitis at P17–20. This suggests that TAK1 is important not only for preventing TNF-induced tissue damage but also for intestinal integrity that is regulated through a TNF independent mechanism. One possibility is involvement of other TNF family receptor ligands such as TRAIL (tumor necrosis factor-related apoptosis-inducing ligand) and FasL, which could also initiate an intracellular apoptotic signaling pathway. TNF, TRAIL and FasL share the same apoptosis-signaling pathway (32). Our preliminary results demonstrate that TAK1 deficiency in keratinocytes, skin epithelial cells, increases sensitivity not only to TNF but also to TRAIL and FasL. TRAIL and FasL may be responsible for inflammation in TAK1-deficient enterocytes.

Alternatively, this delayed inflammatory condition may be caused by increased susceptibility to bacterial invasion due to reduced innate immune responses in TAK1 deficient enterocytes. TAK1 has been shown to be essential for production of cytokines/chemokines, which prevent tissue damage, in response to TLRs and NOD2 activation (1,10). Impairment of commensal bacteria-induced innate immunity in the intestine could enhance intestinal epithelial damage (33). Therefore, it is likely that TAK1 deficient enterocytes do not fully respond to commensal bacteria, and this may contribute to the development of ileitis and colitis. We propose that TAK1 signaling is essential to maintain intestinal homeostasis through induction of cytoprotective genes in enterocytes. Further studies will be necessary to determine the molecular mechanism of TNF-dependent and independent TAK1-mediated cytoprotective function in the intestine.

TAK1 is known to be involved in TGF-β and Wnt signaling pathways (34–37), and could participate in the epithelial development and renewal. Although enterocyte's differentiation is largely normal in TAK1 deficient enterocytes, we cannot rule out the possibility that TAK1 deletion partially impairs cell proliferation/differentiation and causes ileitis and colitis at P17–20. Additionally, cytokine- and bacteria-mediated barrier function may be impaired in enterocyte-derived TAK1 deficient mice causing a dysregulated translocation of luminal antigens and development of ileitis and colitis. Regardless of the mechanism of action, our findings identify enterocyte-derived TAK1 signaling as a critical component of intestinal homeostasis and consequently as a potential therapeutic target for intestinal inflammatory disorders.

Acknowledgments

We thank R. Coffey and G. Bogatcheva for mouse transfer, B.J. Welker and M. Mattmuler for support.

This work was supported by grants from Association pour la Recherche contre le Cancer 3148 and Institut National du Cancer PL 043 to S.R., from National Institutes of Health (DK47700) to C.J., and from Crohn's and Colitis Foundation of America and from National Institutes of Health (GM068812) to J. N-T.

References

1. Akira S, Uematsu S, Takeuchi O. Pathogen Recognition and Innate Immunity. Cell. 2006; 124:783–801. [PubMed: 16497588]
2. Raz E. Organ-specific regulation of innate immunity. Nat. Immunol. 2007; 8:3–4. [PubMed: 17179960]
3. Macpherson AJ, Harris NL. Interactions between commensal intestinal bacteria and the immune system. Nat. Rev. Immunol. 2004; 4:478–485. [PubMed: 15173836]
4. O'Hara AM, Shanahan F. The gut flora as a forgotten organ. EMBO Rep. 2006; 7:688–693. [PubMed: 16819463]
5. Bouma G, Strober W. The immunological and genetic basis of inflammatory bowel disease. Nat. Rev. Immunol. 2003; 3:521–533. [PubMed: 12876555]
6. Xavier RJ, Podolsky DK. Unravelling the pathogenesis of inflammatory bowel disease. 2007; 448:427–434.
7. Ninomiya-Tsuji J, Kishimoto K, Hiyama A, Inoue J, Cao Z, Matsumoto K. The kinase TAK1 can activate the NIK-I κB as well as the MAP kinase cascade in the IL-1 signalling pathway. Nature. 1999; 398:252–256. [PubMed: 10094049]
8. Sato S, Sanjo H, Tsujimura T, Ninomiya-Tsuji J, Yamamoto M, Kawai T, Takeuchi O, Akira S. TAK1 is indispensable for development of T cells and prevention of colitis by the generation of regulatory T cells. Int. Immunol. 2006; 18:1405–1411. [PubMed: 16940043]
9. Shim JH, Xiao C, Paschal AE, Bailey ST, Rao P, Hayden MS, Lee KY, Bussey C, Steckel M, Tanaka N, Yamada G, Akira S, Matsumoto K, Ghosh S. TAK1, but not TAB1 or TAB2, plays an essential role in multiple signaling pathways in vivo. Genes Dev. 2005; 19:2668–2681. [PubMed: 16260493]
10. Kim J-Y, Omori E, Matsumoto K, Nunez G, Ninomiya-Tsuji J. TAK1 is a central mediator of NOD2 signaling in epidermal cells. J. Biol. Chem. 2007; 283:137–144. [PubMed: 17965022]
11. Omori E, Matsumoto K, Sanjo H, Sato S, Akira S, Smart RC, Ninomiya-Tsuji J. TAK1 is a master regulator of epidermal homeostasis involving skin inflammation and apoptosis. J. Biol. Chem. 2006; 281:19610–19617. [PubMed: 16675448]
12. Aggarwal BB. Signalling pathways of the TNF superfamily: a double-edged sword. Nat. Rev. Immunol. 2003; 3:745–756. [PubMed: 12949498]
13. Marini M, Bamias G, Rivera-Nieves J, Moskaluk CA, Hoang SB, Ross WG, Pizarro TT, Cominelli F. TNF-α neutralization ameliorates the severity of murine Crohn's-like ileitis by abrogation of intestinal epithelial cell apoptosis. Proc. Natl. Acad. Sci. U S A. 2003; 100:8366–8371. [PubMed: 12832622]
14. Karin M, Lin A. NF-κ B at the crossroads of life and death. Nat. Immunol. 2002; 3:221–227. [PubMed: 11875461]
15. Feldmann M, Maini RN. Anti-TNFα; THERAPY OF RHEUMATOID ARTHRITIS: What Have We Learned? Annu. Rev. Immunol. 2001; 19:163–196. [PubMed: 11244034]
16. Yan F, John SK, Wilson G, Jones DS, Washington MK, Polk DB. Kinase suppressor of Ras-1 protects intestinal epithelium from cytokine-mediated apoptosis during inflammation. J. Clin. Invest. 2004; 114:1272–1280. [PubMed: 15520859]
17. Sato S, Sanjo H, Takeda K, Ninomiya-Tsuji J, Yamamoto M, Kawai T, Matsumoto K, Takeuchi O, Akira S. Essential function for the kinase TAK1 in innate and adaptive immune responses. Nat. Immunol. 2005; 6:1087–1095. [PubMed: 16186825]
18. Madison BB, Dunbar L, Qiao XT, Braunstein K, Braunstein E, Gumucio DL. Cis elements of the villin gene control expression in restricted domains of the vertical (crypt) and horizontal (duodenum, cecum) axes of the intestine. J. Biol. Chem. 2002; 277:33275–33283. [PubMed: 12065599]
19. El Marjou F, Janssen KP, Chang BH, Li M, Hindie V, Chan L, Louvard D, Chambon P, Metzger D, Robine S. Tissue-specific and inducible Cre-mediated recombination in the gut epithelium. Genesis. 2004; 39:186–193. [PubMed: 15282745]
20. Pfeffer K, Matsuyama T, Kundig TM, Wakeham A, Kishihara K, Shahinian A, Wiegmann K, Ohashi PS, Kronke M, Mak TW. Mice deficient for the 55 kd tumor necrosis factor receptor are

resistant to endotoxic shock, yet succumb to L. monocytogenes infection. Cell. 1993; 73:457–467. [PubMed: 8387893]

21. Sellon RK, Tonkonogy S, Schultz M, Dieleman LA, Grenther W, Balish E, Rennick DM, Sartor RB. Resident enteric bacteria are necessary for development of spontaneous colitis and immune system activation in interleukin-10-deficient mice. Infect. Immun. 1998; 66:5224–5231. [PubMed: 9784526]
22. Athman, R.; Niewohner, J.; Louvard, D.; Robine, S. Epithelial cells: establishment of primary cultures and immortalization. In: Zychlinsky, PSaA, editor. Molecular Cellular Microbiology. New York: Academic Press; 2002. p. 93-113.
23. Nenci A, Becker C, Wullaert A, Gareus R, van Loo G, Danese S, Huth M, Nikolaev A, Neufert C, Madison B, Gumucio D, Neurath MF, Pasparakis M. Epithelial NEMO links innate immunity to chronic intestinal inflammation. Nature. 2007; 446:557–561. [PubMed: 17361131]
24. Jadrich JL, O'Connor MB, Coucouvanis E. The TGF beta activated kinase TAK1 regulates vascular development in vivo. Development. 2006; 133:1529–1541. [PubMed: 16556914]
25. Liu HH, Xie M, Schneider MD, Chen ZJ. Essential role of TAK1 in thymocyte development and activation. Proc. Natl. Acad. Sci. USA. 2006; 103:11677–11682. [PubMed: 16857737]
26. Wan YY, Chi H, Xie M, Schneider MD, Flavell RA. The kinase TAK1 integrates antigen and cytokine receptor signaling for T cell development, survival and function. Nat. Immunol. 2006; 7:851–858. [PubMed: 16799562]
27. Papa S, Bubici C, Zazzeroni F, Pham CG, Kuntzen C, Knabb JR, Dean K, Franzoso G. The NF-κB-mediated control of the JNK cascade in the antagonism of programmed cell death in health and disease. Cell Death Differ. 2006; 13:712–729. [PubMed: 16456579]
28. Li ZW, Chu W, Hu Y, Delhase M, Deerinck T, Ellisman M, Johnson R, Karin M. The IKKbeta subunit of IκB kinase (IKK) is essential for nuclear factor κB activation and prevention of apoptosis. J. Exp. Med. 1999; 189:1839–1845. [PubMed: 10359587]
29. Li Q, Van Antwerp D, Mercurio F, Lee KF, Verma IM. Severe liver degeneration in mice lacking the IκB kinase 2 gene. Science. 1999; 284:321–325. [PubMed: 10195897]
30. Rudolph D, Yeh WC, Wakeham A, Rudolph B, Nallainathan D, Potter J, Elia AJ, Mak TW. Severe liver degeneration and lack of NF-κB activation in NEMO/IKKγ-deficient mice. Genes Dev. 2000; 14:854–862. [PubMed: 10766741]
31. Nenci A, Huth M, Funteh A, Schmidt-Supprian M, Bloch W, Metzger D, Chambon P, Rajewsky K, Krieg T, Haase I, Pasparakis M. Skin lesion development in a mouse model of incontinentia pigmenti is triggered by NEMO deficiency in epidermal keratinocytes and requires TNF signaling. Hum. Mol. Genet. 2006; 15:531–542. [PubMed: 16399796]
32. Ashkenazi A. Targeting death and decoy receptors of the tumour-necrosis factor superfamily. Nat. Rev. Cancer. 2002; 2:420–430. [PubMed: 12189384]
33. Rakoff-Nahoum S, Paglino J, Eslami-Varzaneh F, Edberg S, Medzhitov R. Recognition of commensal microflora by toll-like receptors is required for intestinal homeostasis. Cell. 2004; 118:229–241. [PubMed: 15260992]
34. Hanafusa H, Ninomiya-Tsuji J, Masuyama N, Nishita M, Fujisawa J-i, Shibuya H, Matsumoto K, Nishida E. Involvement of the p38 Mitogen-activated Protein Kinase Pathway in Transforming Growth Factor-beta -induced Gene Expression. J. Biol. Chem. 1999; 274:27161–27167. [PubMed: 10480932]
35. Ishitani T, Kishida S, Hyodo-Miura J, Ueno N, Yasuda J, Waterman M, Shibuya H, Moon RT, Ninomiya-Tsuji J, Matsumoto K. The TAK1-NLK mitogen-activated protein kinase cascade functions in the Wnt-5a/Ca(2+) pathway to antagonize Wnt/β-catenin signaling. Mol. Cell. Biol. 2003; 23:131–139. [PubMed: 12482967]
36. Ishitani T, Ninomiya-Tsuji J, Nagai S, Nishita M, Meneghini M, Barker N, Waterman M, Bowerman B, Clevers H, Shibuya H, Matsumoto K. The TAK1-NLK-MAPK-related pathway antagonizes signalling between β-catenin and transcription factor TCF. Nature. 1999; 399:798–802. [PubMed: 10391247]
37. Kajino T, Omori E, Ishii S, Matsumoto K, Ninomiya-Tsuji J. TAK1 MAPK kinase kinase mediates transforming growth factor-beta signaling by targeting SnoN oncoprotein for degradation. J Biol Chem. 2007; 282:9475–9481. [PubMed: 17276978]

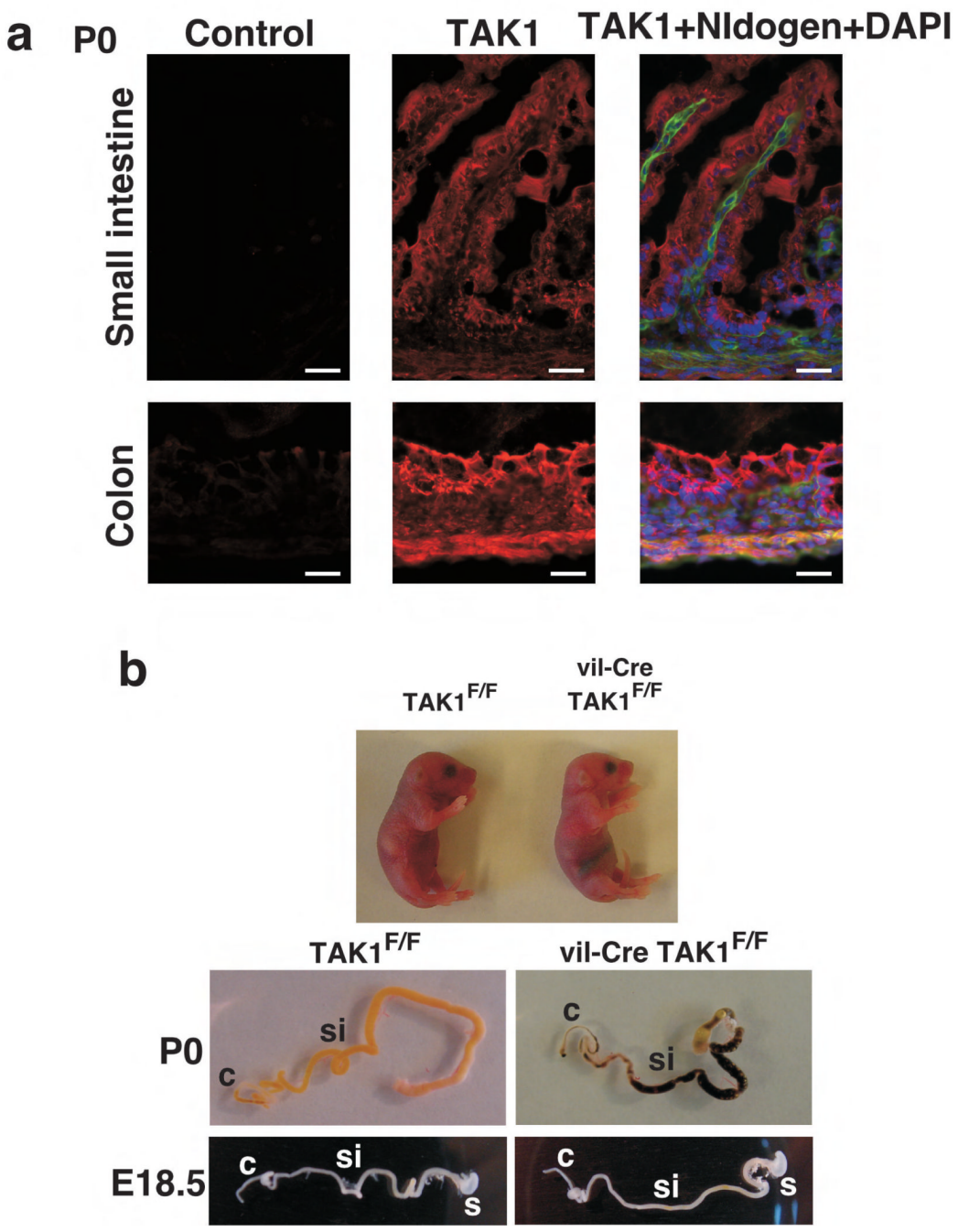

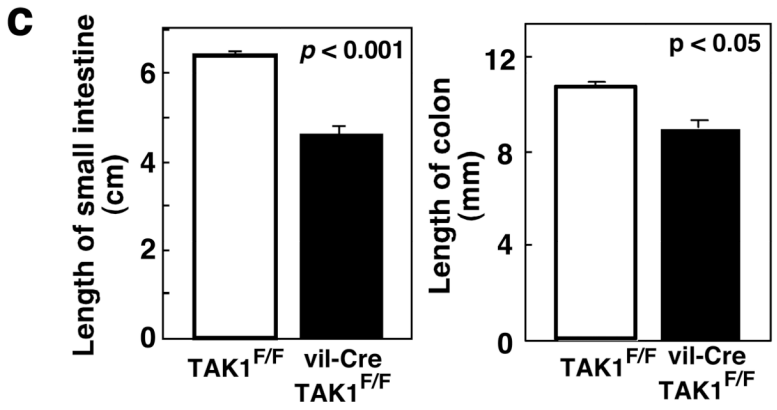

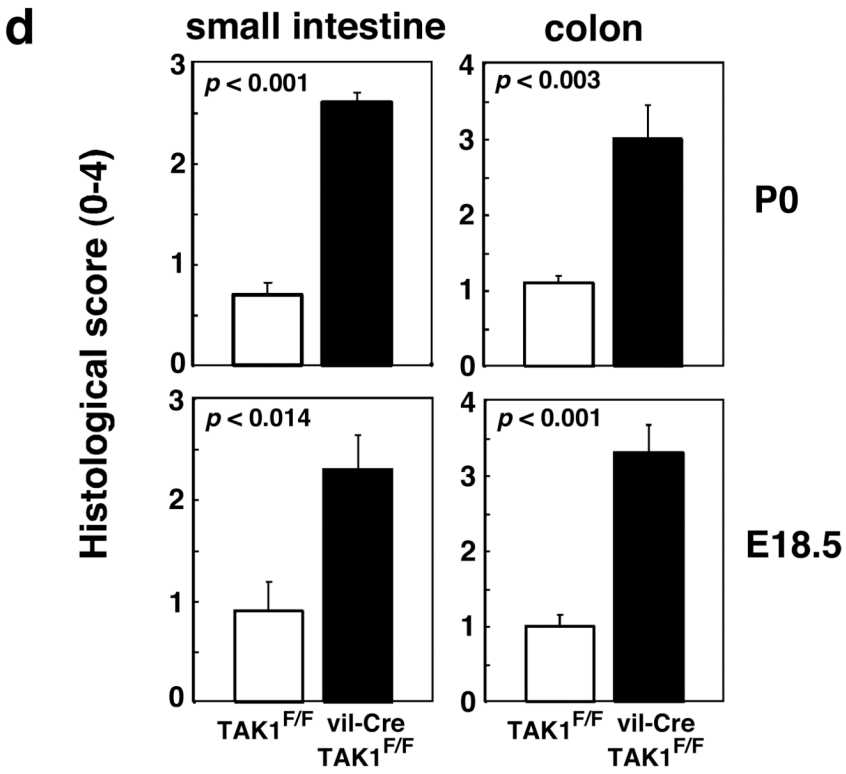

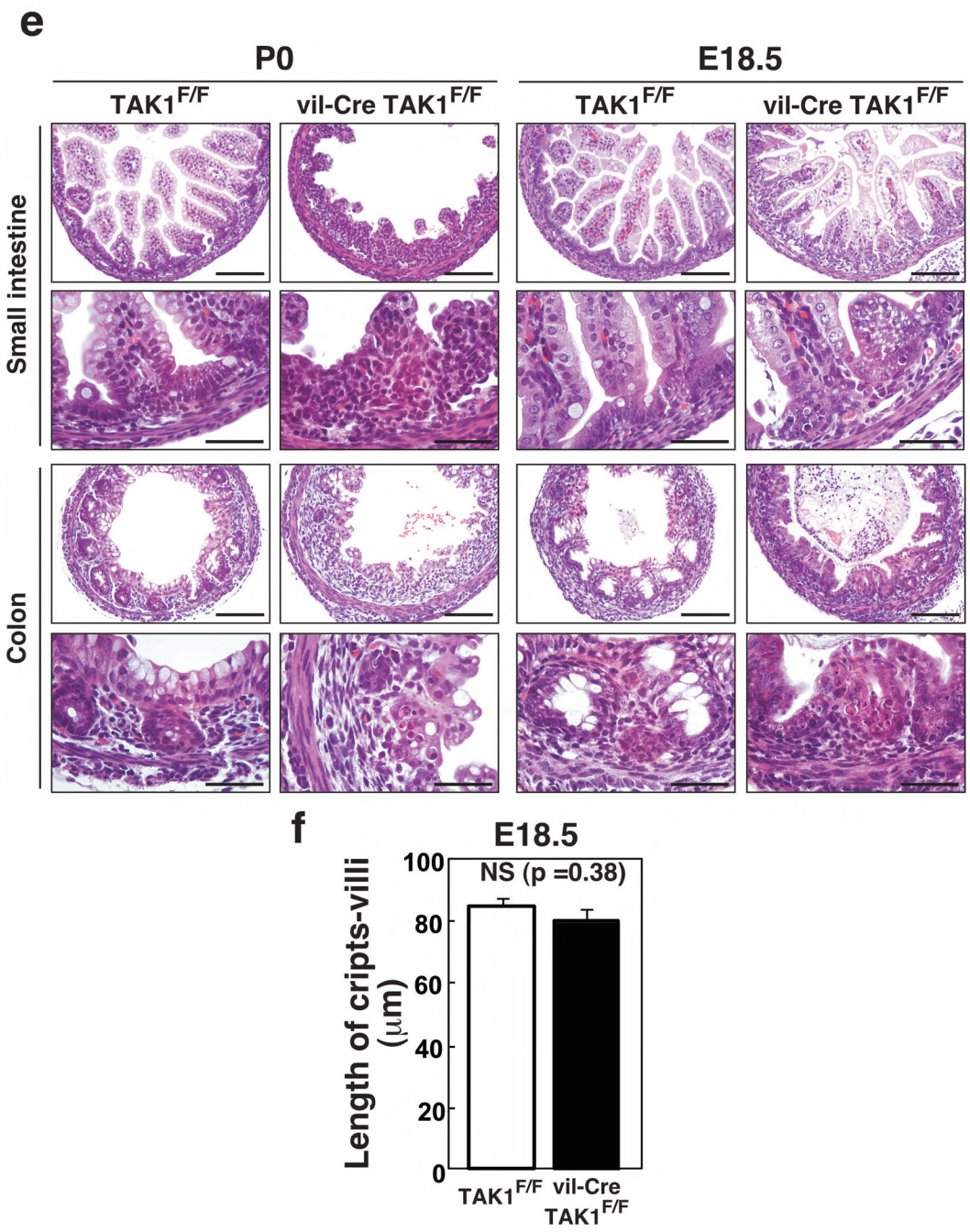

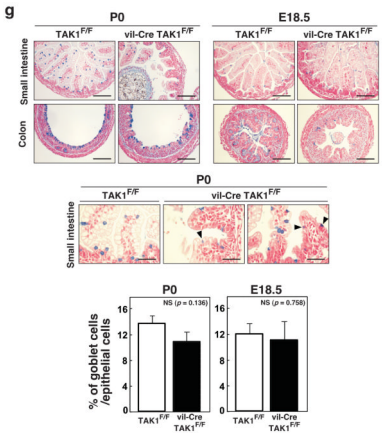

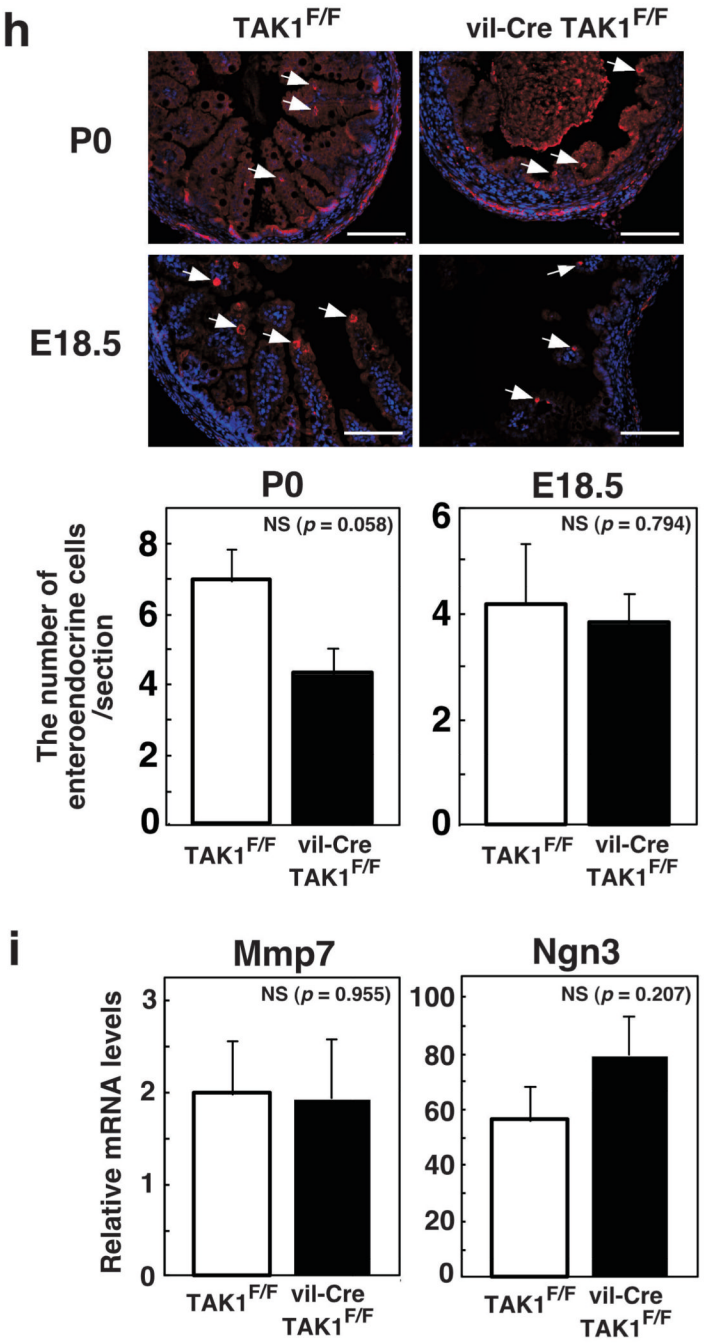

Figure 1. TAK1 is ubiquitously expressed and enterocytes-specific TAK1 deletion causes intestinal damage

(a) Sections of the small intestine and colon from P0 control *TAK1*$^{FL/FL}$ mouse were immunostained with control rabbit IgG (control), or anti-TAK1 (TAK1) along with anti-Nidgen antibody and DAPI. Control rabbit IgG and TAK1 are red and Nidgen is green. Blue indicates nuclei stained with DAPI. Scale bars, 50 μm.

(b) Control *TAK1*$^{FL/FL}$ (TAK1$^{F/F}$) and *villin-CreTAK1*$^{FL/FL}$ (vil-CreTAK1$^{F/F}$) mice at P0 (top panels). The intestine of control and *villin-CreTAK1*$^{FL/FL}$ mice at P0 and E18.5 (middle and bottem panels).

(c) The length of small intestine (left panel) and colon (right panel) of control *TAK1*$^{FL/FL}$ (TAK1$^{F/F}$, open bars) and *villin-CreTAK1*$^{FL/FL}$ (vil-CreTAK1$^{F/F}$, filled bars) mice at P0. Data show the means ± S.E. (*TAK1*$^{FL/FL}$, n=46; *villin-CreTAK1*$^{FL/FL}$, n=26). The results of student t test (P) are shown above the graph.
(d) Histological scores from control (TAK1$^{F/F}$) and *villin-CreTAK1*$^{FL/FL}$ (vil-CreTAK1$^{F/F}$) mice at P0 and E18.5. Data show the means ± S.E. and the P values (student t test) (n=5).
(e) Small intestinal and colonic sections from control (TAK1$^{F/F}$) and *villin-CreTAK1*$^{FL/FL}$ (vil-CreTAK1$^{F/F}$) mice at P0 and E18.5 were stained with hematoxylin/eosin. Scale bars, 50 μm in low magnification, 20 μm in high magnification.
(f) The length of cripts-villi axes of control (TAK1$^{F/F}$, open bars) and *villin-CreTAK1* $^{FL/FL}$ (vil-CreTAK1$^{F/F}$, filled bars) mice at E18.5. Data show the means ± S.E. (*TAK1*$^{FL/FL}$; n=18, *villin-CreTAK1*$^{FL/FL}$; n=10). NS, not significant
(g) Alcian Blue staining for identifying goblet cells in the small intestine and the colon from control (TAK1$^{F/F}$) and *villin-CreTAK1*$^{FL/FL}$ (vil-CreTAK1$^{F/F}$) mice at P0 and E18.5. Goblet cells were stained with blue. Arrows indicate smaller goblet cells. Scale bars, 50 μm (top and middle panels), 25 μm (bottom panels). The percentages of goblet cells of the total enterocytes in the small intestine at P0 (*TAK1*$^{FL/FL}$, n=17; *villin-CreTAK1*$^{FL/FL}$, n=16) and E18.5 (*TAK1*$^{FL/FL}$, n=20; *villin-CreTAK1*$^{FL/FL}$, n=12) were shown. Data show the means ± S.E. NS, not significant.
(h) Small intestinal sections from control *TAK1*$^{FL/FL}$ (TAK1$^{F/F}$) and *villin-CreTAK1*$^{FL/FL}$ (vil-CreTAK1$^{F/F}$) mice at P0 and E18.5 were immunostained with anti-Synaptophysin (red). Blue indicates nuclei stained with DAPI. Arrows indicate enteroendocrine cells. Scale bars, 50 μm. The number of enteroendocrine cells in the small intestine at P0 (*TAK1*$^{FL/FL}$, n=12; *villin-CreTAK1*$^{FL/FL}$, n=7) and E18.5 (*TAK1*$^{FL/FL}$, n=6; *villin-CreTAK1*$^{FL/FL}$, n=5) were shown. Data show the means ± S.E. NS, not significant.
(i) RNAs were isolated from the small intestine of control *TAK1*$^{FL/FL}$ (TAK1 $^{F/F}$, open bars) and *villin-CreTAK1*$^{FL/FL}$ (vil-CreTAK1$^{F/F}$, filled bars) at E18.5. Real-time PCR analysis was performed to quantify paneth cell marker: Mmp7 and enteroendocrine cell marker: Ngn3 expression levels. Relative mRNA levels were calculated using GAPDH mRNAs. Data show the means ± S.E. (*TAK1*$^{FL/FL}$, n=11; *villin-CreTAK1*$^{FL/FL}$, n=10). NS, not significant.

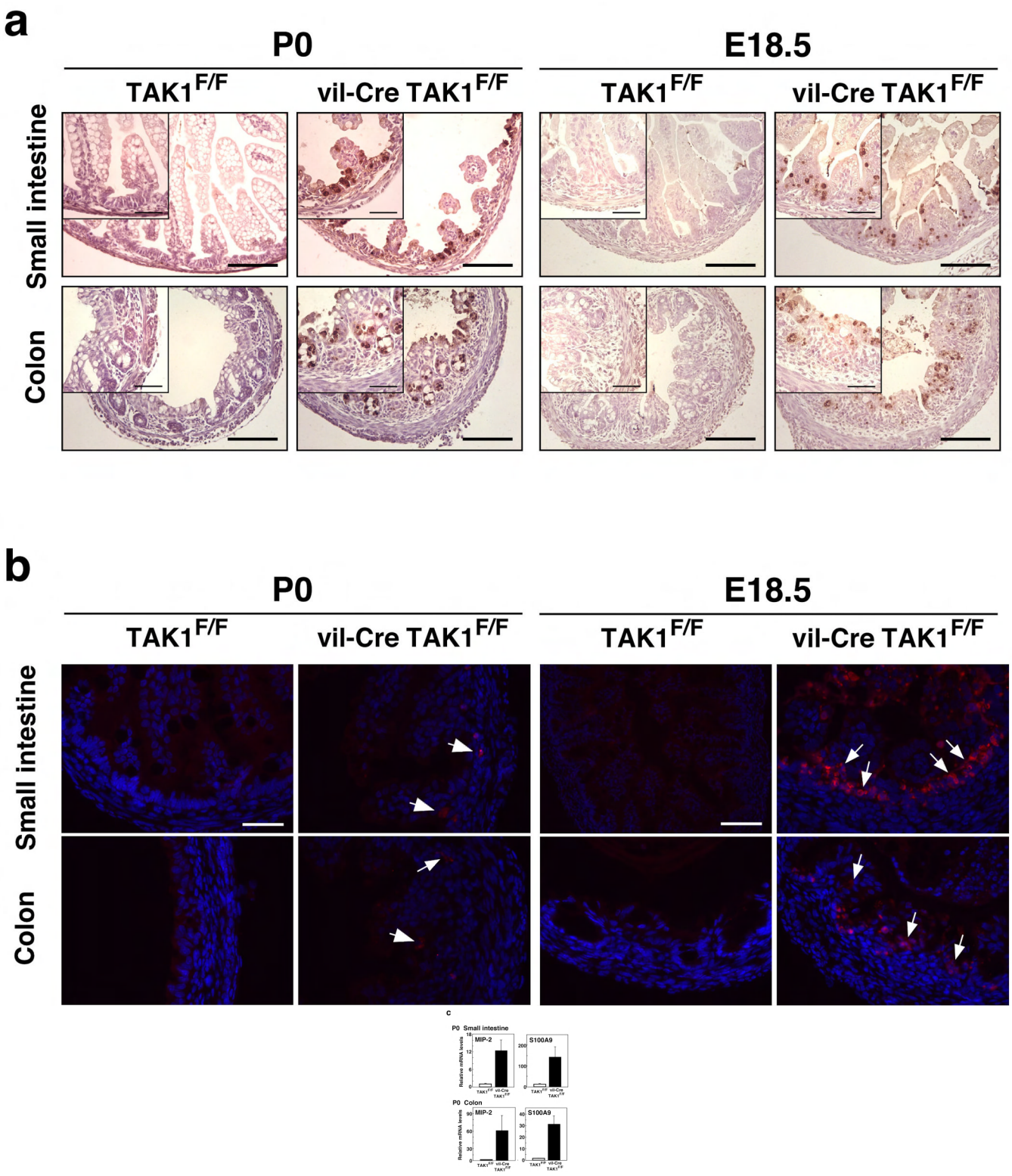

Figure 2. TAK1 deletion causes apoptosis and inflammation at E18.5-P0

(a) TUNEL assay was performed on small intestinal and colonic sections of control (TAK1 $^{F/F}$) and *villin-CreTAK1*$^{FL/FL}$ (vil-CreTAK1$^{F/F}$) mice at P0 and E18.5. Scale bars, 50 μm in low magnification, 20 μm in high magnification.
(b) Small intestinal and colonic sections from control *TAK1*$^{FL/FL}$ (TAK1$^{F/F}$) and *villin-CreTAK1*$^{FL/FL}$ (vil-CreTAK1$^{F/F}$) mice at P0 and E18.5 were immunostained with anti-Cleaved Caspase-3 antibody (red). Blue indicates nuclei stained with DAPI. Arrows indicate examples of apoptotic cells. Scale bars, 20 mm.
(c) Quantification of mRNA levels in the control (TAK1$^{F/F}$) and *villin-CreTAK1*$^{FL/FL}$ (vil-CreTAK1$^{F/F}$, filled bars) small intestine and colon at P0 by real-time PCR. mRNA levels relative to GAPDH mRNA are shown. In P0 small intestine, data show the means ± S.E. (*TAK1*$^{FL/FL}$, n=27; *villin-CreTAK1*$^{FL/FL}$, n=14; MIP-2, $p < 0.009$; S100A9, $p < 0.02$), and in P0 colon, data show the means ± S.E. (*TAK1*$^{FL/FL}$, n=11; *villin-CreTAK1*$^{FL/FL}$, n=8; MIP-2, $p < 0.092$; S100A9, $p < 0.05$).

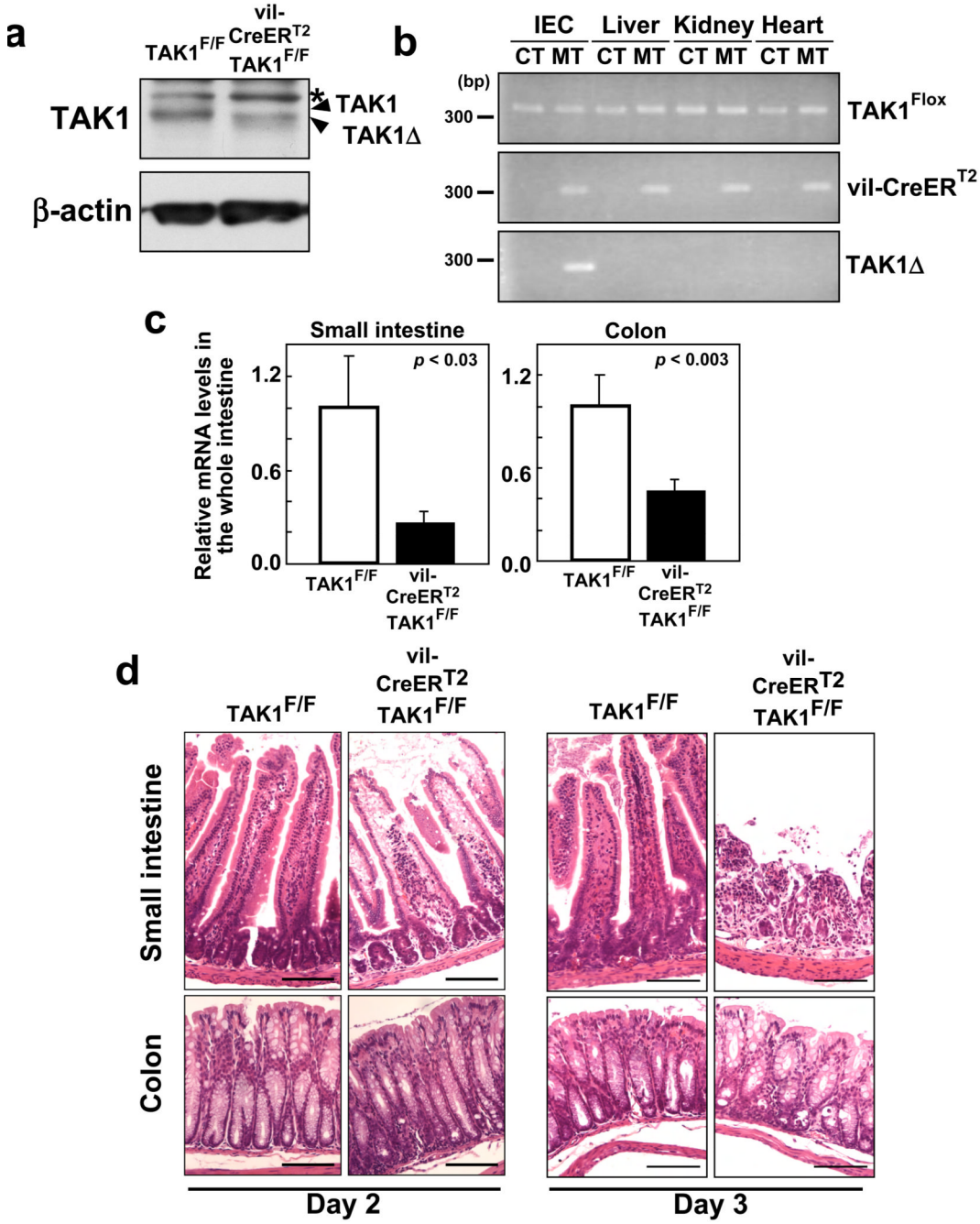

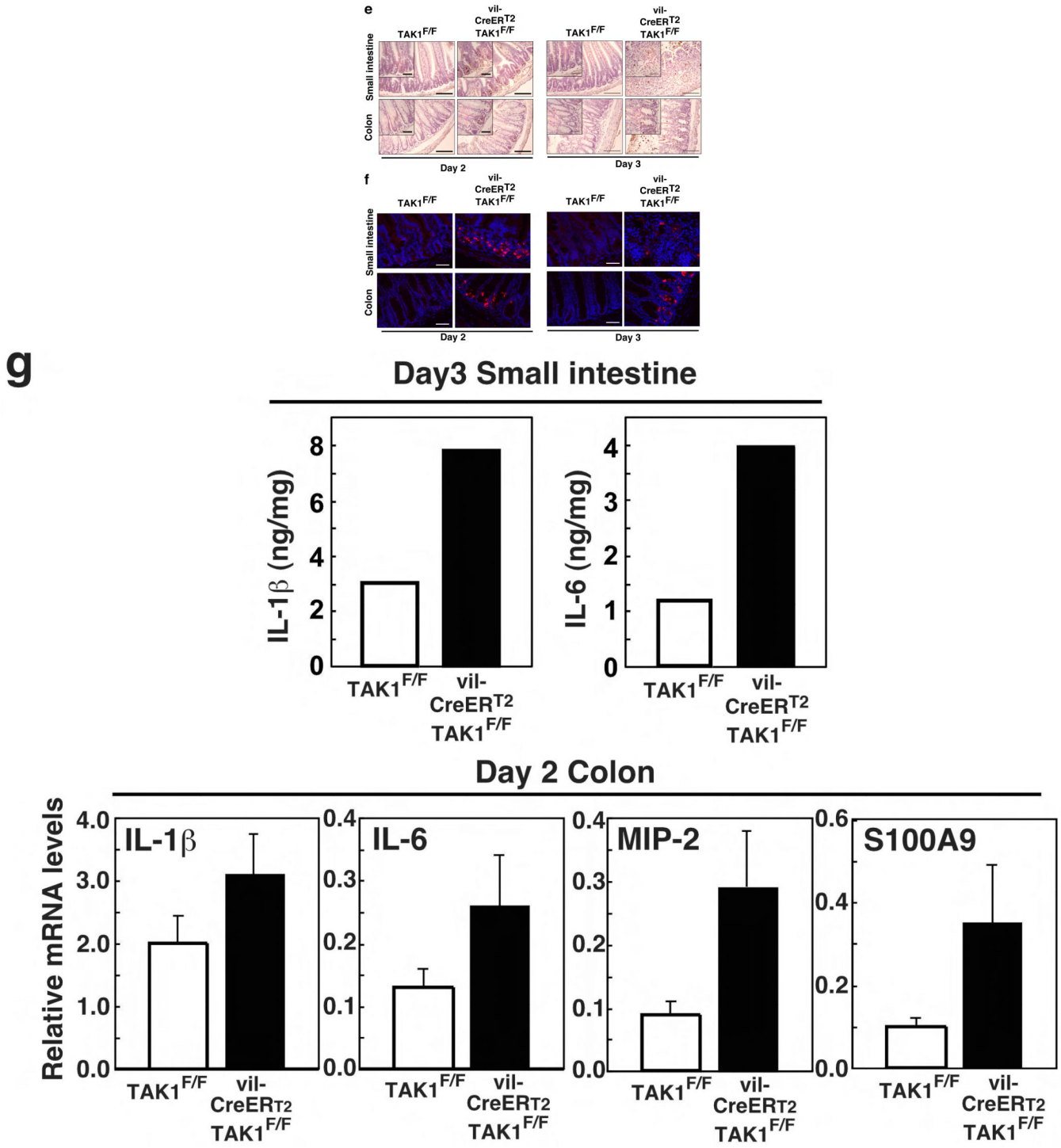

Figure 3. TAK1 is required for prevention of apoptosis and inflammation in 4-week-old mice

(a) Control ($TAK1^{F/F}$) and *villin-CreER^{T2}TAK1$^{FL/FL}$* (vil-$CreER^{T2}TAK1^{F/F}$) 4-week-old mice were injected with tamoxifen for 2 days. Immunoblot analysis of TAK1 in enterocytes. β-actin was used as a loading control. Asterisk indicates non-specific band.

(b) Genomic PCR analysis for floxed TAK1 ($TAK1^{Flox}$), villin-$CreER^{T2}$ (vil-$CreER^{T2}$) and truncated TAK1 (TAK1Δ) in enterocytes (intestinal epithelial cell (IEC)), liver, kidney and

heart of control *TAK1*$^{FL/FL}$ (CT) and *villin-CreER*^{T2}*TAK1*$^{FL/FL}$ (MT) mice injected with tamoxifen for 2 days.

(c) Real-time PCR analysis to quantify full-length TAK1 mRNA levels isolated from the whole small intestine and colon. Relative mRNA levels were calculated using GAPDH mRNAs. Data show the means ± S.E. (Small intestine, *TAK1*$^{FL/FL}$, n=8; *villin-CreER*^{T2} *TAK1*$^{FL/FL}$, n=9, Colon, TAK1$^{FL/FL}$, n=8; *villin-CreER*^{T2} *TAK1*$^{FL/FL}$, n=9).

(d) Small intestinal and colonic sections from 4-week-old mice of control (TAK1 $^{F/F}$) and *villin-CreER*^{T2}*TAK1*$^{FL/FL}$ (vil-CreER^{T2}TAK1$^{F/F}$) treated with tamoxifen (Day 2 and Day 3) were stained with hematoxylin/eosin. Scale bars, 50 μm.

(e) TUNEL staining of small intestinal and colonic sections from 4-week-old mice of control *TAK1*$^{FL/FL}$ (TAK1 $^{F/F}$) and *villin-CreER*^{T2}*TAK1*$^{FL/FL}$ (vil-CreER^{T2}TAK1$^{F/F}$) treated with tamoxifen (Day 2 and Day 3). Scale bars, 50 μm in low magnification, 20 μm in high magnification.

(f) Small intestinal and colonic sections from 4-weeks-old mice of control *TAK1*$^{FL/FL}$ (TNFR1$^{F/F}$) and *villin-CreER*^{T2}*TAK1*$^{FL/FL}$ (vil-CreER^{T2}TAK1$^{F/F}$) with tamoxifen treatment for 2 days (Day 2) and for 3 days (Day 3) were stained with anti-Cleaved Caspase-3 antibody (red). Blue indicates nuclei stained with DAPI. Scale bars, 20 μm.

(g) (left panels) Productions of IL-1β and IL-6 in the small intestines from TAK1$^{FL/FL}$ (TAK1$^{F/F}$, open bars) and villin-CreTAK1$^{FL/FL}$ (vil-CreTAK1$^{F/F}$, filled bars) mice injected with tamoxifen for 3 days at 4-week-old. Data are representative of three independent experiments. (right paneles) Real-time PCR analysis was performed in colon from control (TAK1$^{F/F}$, open bars) and *villin-CreER*^{T2}*TAK1*$^{FL/FL}$ (vil-CreER^{T2}TAK1$^{F/F}$, filled bars) mice treated with tamoxifen (Day 2). mRNA levels relative to GAPDH mRNA are shown. Day 2, TAK1$^{FL/FL}$, n=6; *villin-CreER*^{T2}*TAK1*$^{FL/FL}$; IL-1β, $p < 0.15$; IL-6, $p < 0.066$; MIP-2, $p < 0.022$; S100A9, $p < 0.017$.

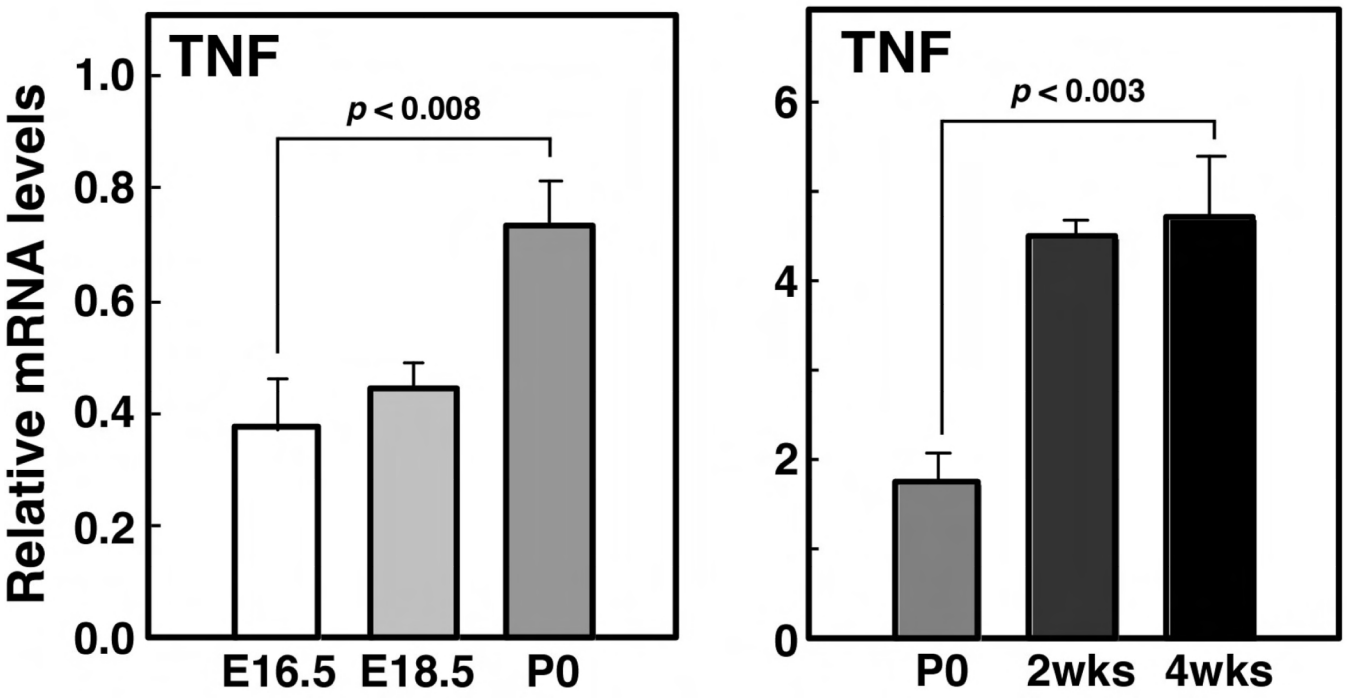

Figure 4. The level of TNF is increased around the time of birth and further as mice grow

TNF mRNA levels in the small intestine at E16.5, E18.5 and P0 (left panel), and at P0, 2-week-old and 4-week-old (right panel) were analyzed by real-time PCR. Because the levels of TNF expression was unaffected by genotype, data from two genotypes, *TAK1*$^{F/F}$ and *TAK1*$^{F/+}$, (left panel) or from three genotypes, *villin-CreER*^{T2}*TAK1*$^{FL/FL}$, *villin-CreER*^{T2}*TAK1*$^{+/+}$ and *villin-CreER*^{T2}*TAK1*$^{FL/+}$ without tamoxifen treatment, (right panel) were combined. mRNA levels from relative to GAPDH mRNA are shown. (left panel, E16.5, n=5; E18.5, n=22; P0, n=27) (right panel, ,P0, n=7; 2-week-old, n=7; 4-week-old, n=7). The results of student t test (P) are shown above the graph.

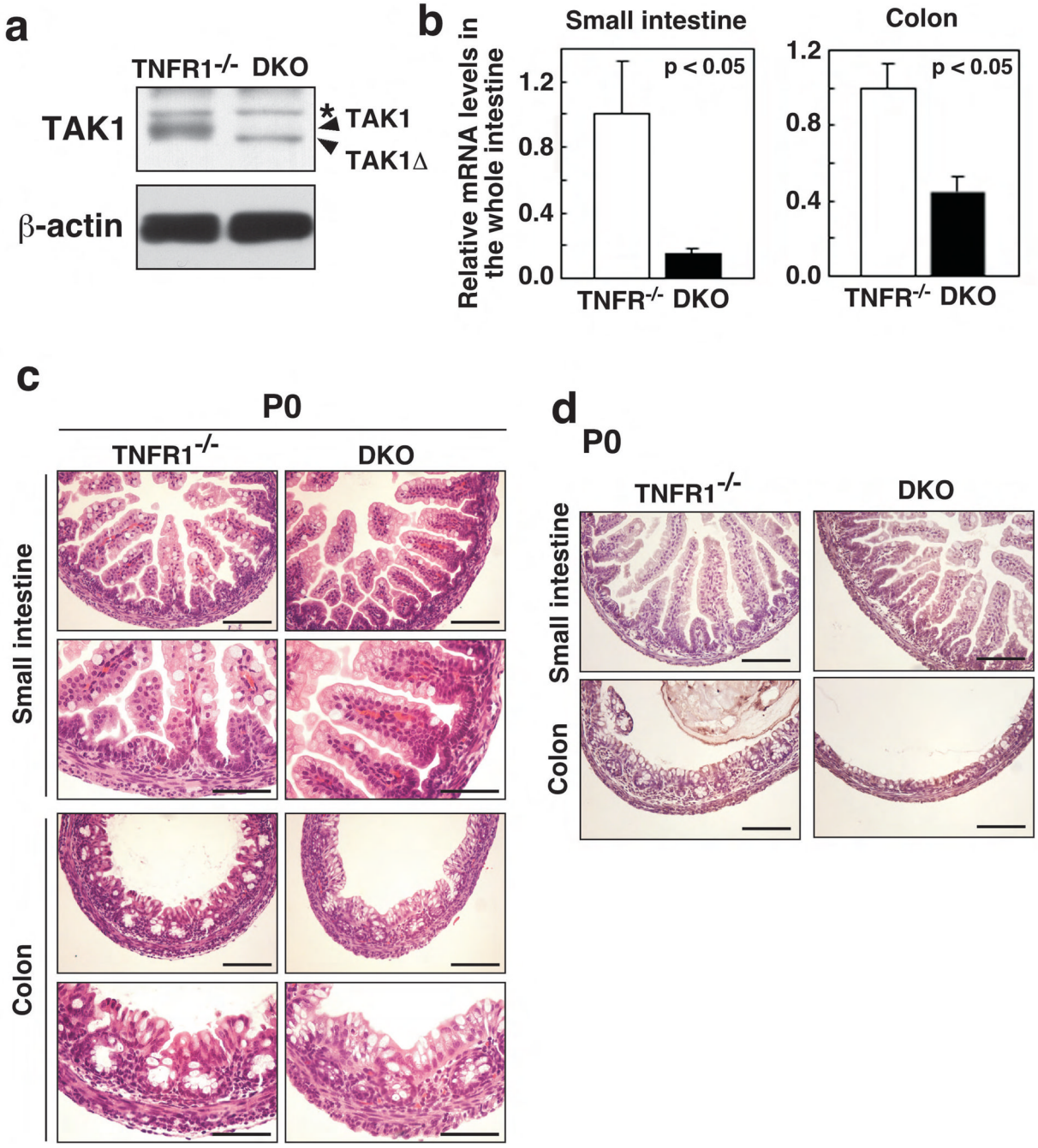

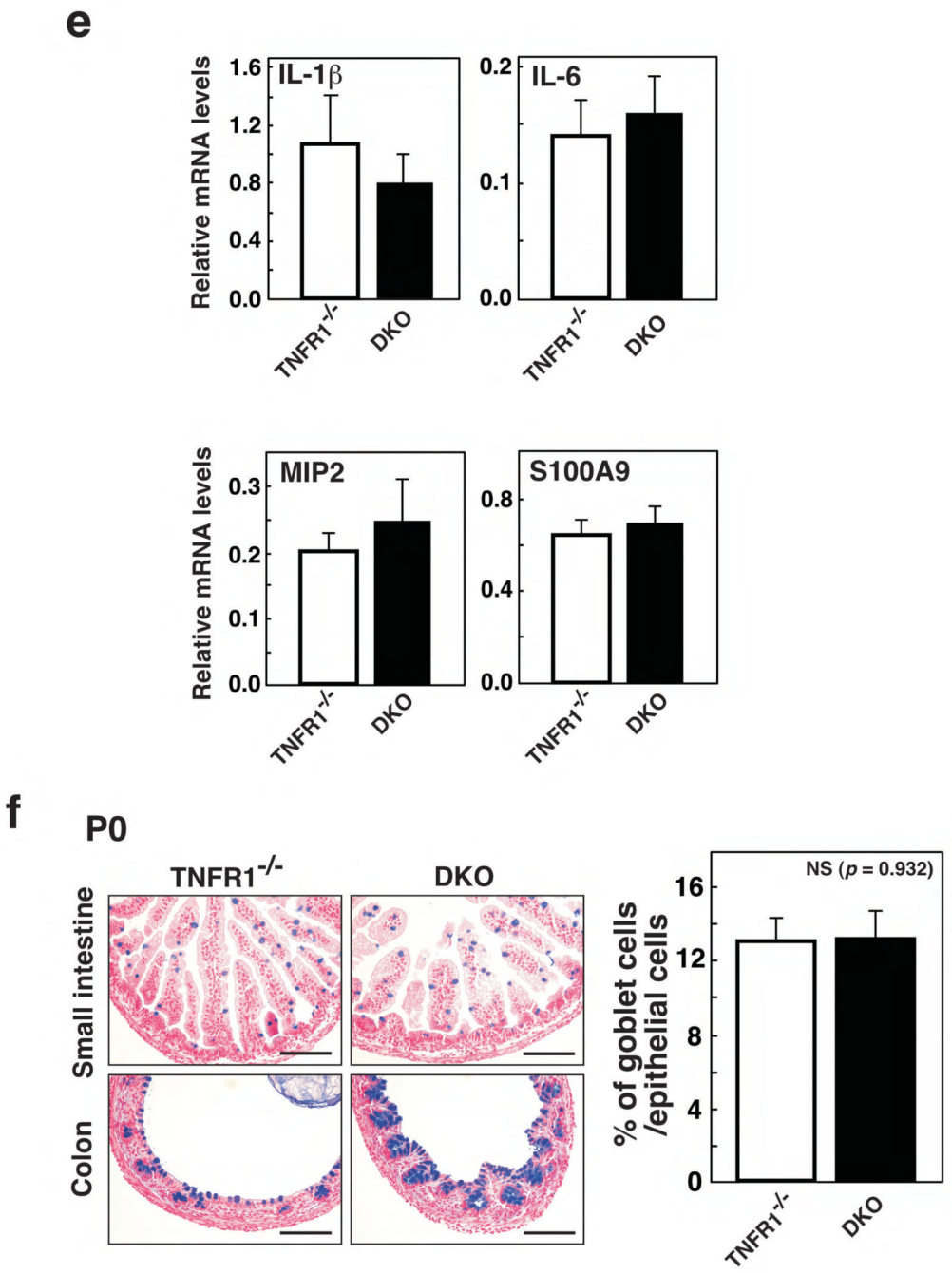

Figure 5. Tissue damage in TAK1 mutant mice is rescued by TNFR1 deletion

(a) TAK1 protein in enterocytes prepared from control *TAK1*$^{FL/FL}$ *TNFR1*$^{-/-}$ (TNFR1$^{-/-}$) and *villin-CreTAK1*$^{FL/FL}$ *TNFR1*$^{-/-}$ (DKO) mice at P15 was analyzed by immunoblotting. β-actin was used as a loading control. Asterisk indicates non-specific band.

(b) Real-time PCR analysis to quantify full-length TAK1 mRNA. RNAs were isolated from control *TAK1*$^{FL/FL}$ *TNFR1*$^{-/-}$ (TNFR$^{-/-}$) and *villin-CreTAK1*$^{FL/FL}$ *TNFR1*$^{-/-}$ (DKO) mice at 2–3 weeks old. mRNA levels relative to GAPDH mRNA are shown. Data show the means ± S.E. (TNFR1$^{-/-}$, n=8; DKO, n=8).

(c) Hematoxylin/eosin staining on sections of small intestine and colon from control *TAK1*$^{FL/FL}$ *TNFR1*$^{-/-}$ (TNFR1$^{-/-}$) and *villin-CreTAK1*$^{FL/FL}$ *TNFR1*$^{-/-}$ (DKO) mice at P0. Scale bars, 50 μm in low magnification, 25 μm in high magnification.
(d) TUNEL assay was performed on small intestinal and colonic sections of control *TAK1*$^{FL/FL}$ *TNFR1*$^{-/-}$ (TNFR1$^{-/-}$) and *villin-CreTAK1*$^{FL/FL}$ *TNFR1*$^{-/-}$ (DKO) mice at P0. Scale bars, 50 μm.
(e) Expression levels of the indicated genes in the control *TAK1*$^{FL/FL}$ *TNFR1*$^{-/-}$ (TNFR1$^{-/-}$, open bars) and *villin-CreTAK1*$^{FL/FL}$ *TNFR1*$^{-/-}$ (DKO, filled bars) small intestine at P0. mRNA levels relative to GAPDH mRNA are shown. TNFR1$^{-/-}$, n=13; DKO, n=11; IL-1β, NS, $p < 0.511$; IL-6, NS, $p < 0.655$; MIP-2, NS, $p < 0.466$; S100A9, NS, $p < 0.603$). NS, not significant.
(f) Alcian Blue staining for identifying goblet cells in the small intestine and the colon from control *TAK1*$^{FL/FL}$ *TNFR1*$^{-/-}$ (TNFR1$^{-/-}$) and *villin-CreTAK1*$^{FL/FL}$ *TNFR1*$^{-/-}$ (DKO) P15 mice. Scale bars, 50 μm. The percentages of goblet cells in the small intestine at P0 (*TAK1*$^{FL/FL}$ *TNFR1*$^{-/-}$, n=18; *villin-CreTAK1*$^{FL/FL}$ *TNFR1*$^{-/-}$, n=18) were shown. Data show the means ± S.E. NS, not significant.

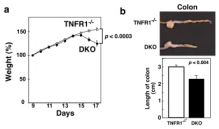

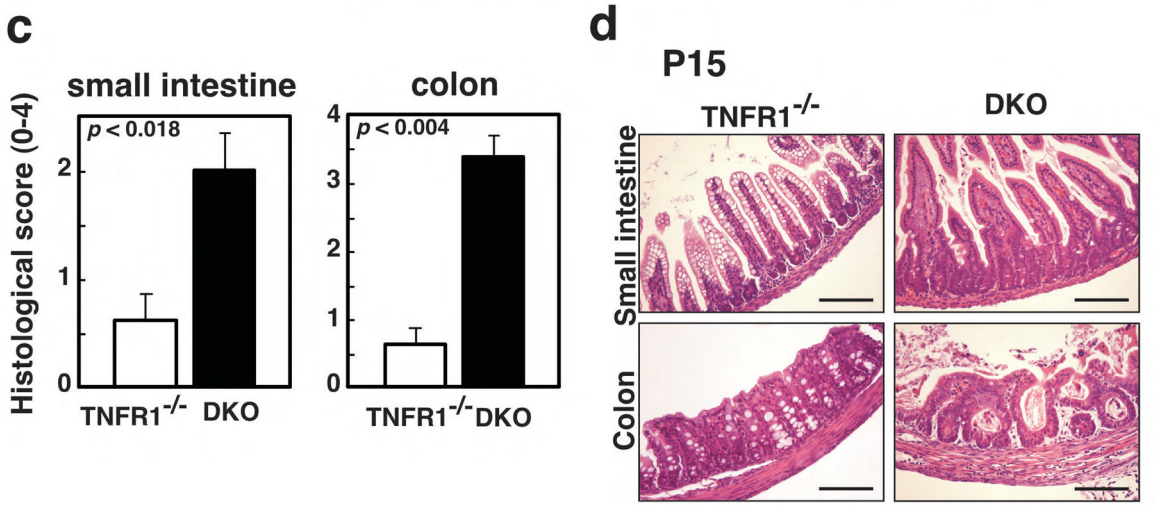

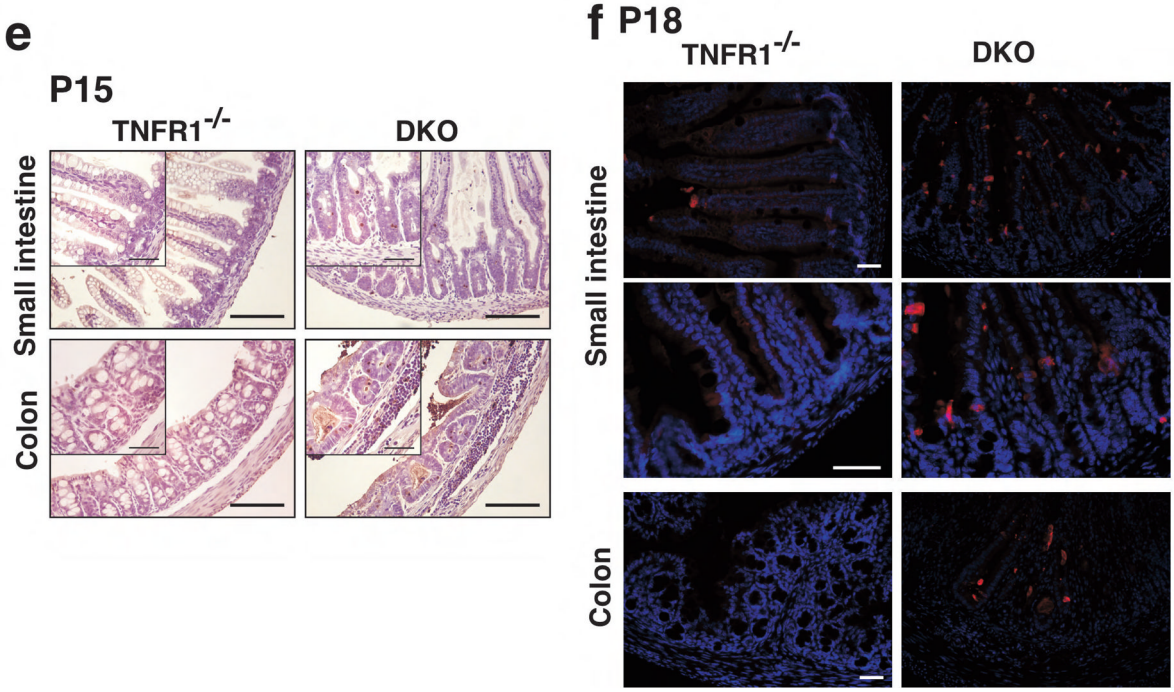

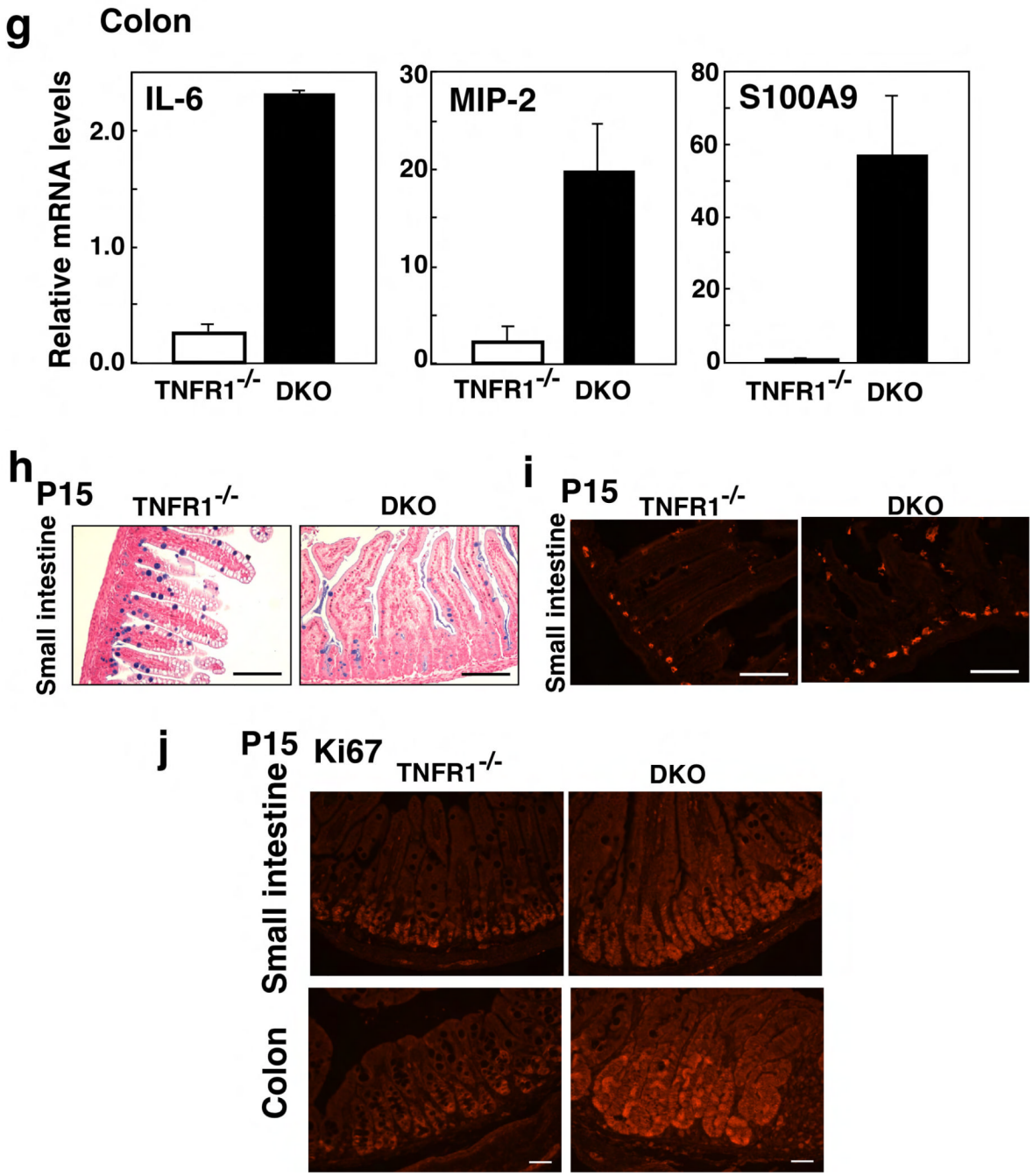

Figure 6. Older double-mutant mice with intestinal epithelium-specific TAK1 deletion and TNFR1 deletion spontaneously develop ileitis and colitis

(a) Percentage of body weight relative to the body weight at P9 of control *TAK1*$^{FL/FL}$ *TNFR1*$^{-/-}$ (TNFR1$^{-/-}$, open circle) and *villin-CreTAK1*$^{FL/FL}$ *TNFR1*$^{-/-}$ (DKO, closed circle) mice. The results show the means ± S.E. and the P value (student t test) at P17 (TNFR1$^{-/-}$, n=19; DKO, n=10)

(b) (left panel) Colons from control and DKO at P16. (right panel) The colon length of control *TAK1*$^{FL/FL}$*TNFR1*$^{-/-}$ (TNFR1$^{-/-}$, open bars) and *villin-CreTAK1*$^{FL/FL}$*TNFR1*$^{-/-}$ (DKO, filled bars) mice at P15–P18. Data show the means ± S.E. and the P value (student t test) (TNFR1−/−, n=9; DKO, n=12).

(c) Histological scores from control *TAK1*$^{FL/FL}$ *TNFR1*$^{-/-}$ (TNFR1$^{-/-}$) and *villin-CreTAK1*$^{FL/FL}$ *TNFR1*$^{-/-}$ (DKO) P15–P18 mice. Data show the means ± S.E. and the P value (student t test) (n=4).
(d) Hematoxylin/eosin staining was performed on sections of the small intestine and the colon from control *TAK1*$^{FL/FL}$ *TNFR1*$^{-/-}$ (TNFR1$^{-/-}$) and *villin-CreTAK1*$^{FL/FL}$ *TNFR1*$^{-/-}$ (DKO) P15 mice. Scale bars, 50 μm.
(e) Sections of control *TAK1*$^{FL/FL}$ *TNFR1*$^{-/-}$ (TNFR1$^{-/-}$) and *villin-CreTAK1*$^{FL/FL}$ *TNFR1*$^{-/-}$ (DKO) P15 mice small intestine and colon were subjected to TUNEL analysis. Scale bars, 50 μm in low magnification, 20 μm in high magnification.
(f) Small intestinal and colonic sections from control *TAK1*$^{FL/FL}$*TNFR1*$^{-/-}$ (TNFR1$^{-/-}$) and villin-CreTAK1$^{FL/FL}$TNFR1−/− (DKO) mice at P18 were immunostained with anti-Cleaved Caspase-3 antibody (red). Blue indicates nuclei stained with DAPI. Scale bars, 20 mm.
(g) Quantification of the indicated gene expression by real-time PCR in the colon harvested from control *TAK1*$^{FL/FL}$ *TNFR1*$^{-/-}$ (TNFR1$^{-/-}$, open bars) and *villin-CreTAK1*$^{FL/FL}$ *TNFR1*$^{-/-}$ (DKO, filled bars) 4-week-old mice. mRNA levels relative to GAPDH mRNA are shown. TNFR1$^{-/-}$, n=8; DKO, n=8; IL-6, $p < 0.036$; MIP-2, $p < 0.008$; S100A9, $p < 0.012$.
(h) Alcian Blue staining in the small intestine and the colon from control *TAK1*$^{FL/FL}$ *TNFR1*$^{-/-}$ (TNFR1$^{-/-}$) and *villin-CreTAK1*$^{FL/FL}$ *TNFR1*$^{-/-}$ (DKO) mice at P15. Goblet cells were stained with blue. Scale bars, 50 μm.
(i) Small intestinal sections from control *TAK1*$^{FL/FL}$ *TNFR1*$^{-/-}$ (TNFR1$^{-/-}$) and *villin-CreTAK1*$^{FL/FL}$ *TNFR1*$^{-/-}$ (DKO) P15 mice were immunostained with anti-Lysozyme (red). The red staining in the bottom of crypts represents paneth cells. The red staining around villus are non-specific staining. Scale bars, 50 μm.
(j) Small intestinal and colonic sections from control *TAK1*$^{FL/FL}$*TNFR1*$^{-/-}$ (TNFR1$^{-/-}$) and *villin-CreTAK1*$^{FL/FL}$*TNFR1*$^{-/-}$ (DKO) mice at P18 were immunostained with anti-Ki67 antibody. Scale bars, 20 μm.

Table 1

Correlation between apoptosis and the levels of inflammatory molecules at E18.5[a]

			IL-1β		IL-6		MIP-2		S100A9	
Genotype	**TUNEL**	**Number of mice**	**Relative mRNA levels**	**Average**	**Relative mRNA levels**	**Average**	**Relative mRNA levels**	**Average**	**Relative mRNA levels**	**Average**
$TAK1^{FL/FL}$	−	7	0.18	0.57	0.1	0.08	0.05	0.08	11.14	3.20
	−		0.37		0.1		0.09		10.32	
	−		0.59		0.04		0.03		0.18	
	−		1.23		0.07		0.17		0.11	
	−		0.62		0.08		0.03		0.22	
	−		0.25		0.01		0.01		0.18	
	−		0.77		0.14		0.15		0.25	
villin-Cre	−	2	0.08	0.20	0.03	0.07	0.02	0.03	1.63	0.90
$TAK1^{FL/FL}$	−		0.31		0.1		0.03		0.17	
	+	2	3.11	1.64	0.07	0.06	0.24	0.15	0.28	0.27
	+		0.17		0.05		0.05		0.25	
	++	3	14.5	37.09	2.56	4.63	14.70	20.28	25.59	99.94
	++		31.08		5.81		17.36		113.59	
	+++		65.70		5.53		28.79		160.64	

[a]More than 6 small intestinal sections with TUNEL staining from each control ($TAK1^{F/F}$) or *villin-CreTAK1*$^{FL/FL}$ (vil-Cre$TAK1^{F/F}$) mouse at E18.5 were scored using the scale of −, +, ++ and +++ (−, no TUNEL positive cell was found; +, TUNEL positive cells were found in scattered area of one or two sections; ++, TUNEL positive cells were found in a large area of more than 70% of sections; +++, TUNEL positive cells were found in a large area of all sections). The RNA samples isolated from the same small intestines were subjected to quantification of mRNA levels. mRNA levels relative to GAPDH mRNA are shown.